Longitudinal Growth of Polymer Crystals from Flowing Solutions. VIII. Mechanism of Fiber Formation on Rotor Surface

J. C. M. TORFS and A. J. PENNINGS, *Laboratory of Polymer Chemistry, State University of Groningen, Nijenborgh 16 9747 AG Groningen, The Netherlands*

Synopsis

A study has been made of the mechanism of the fibrous crystallization process of high-molecular-weight polyethylene from dilute solution subjected to Couette flow. Fiber growth has been observed to take place in a gel layer adhering to the surface of the rotating inner cylinder. The fiber is both taper and ribbonlike shaped, which suggests that growth occurs primarily on the lateral surfaces. The crystal growth rate, as determined by measurements of the fiber cross section, is found to depend on the roughness and the chemical nature of the rotor surface, and is independent of the take-up speed. These observations have led to the following conclusions concerning the mechanism. Long-chain molecules adsorb onto the rotor surface. By reptation an entanglement network is formed. It has long relaxation times due to the tendency of the supercooled chains to form embryonic crystallites upon slight orientation. This network is stretched by the entanglement formation with the cilia of a seed crystal, followed by shear stresses. Stretching will lead to further crystallization. The elastically active chain parts between entanglements will lead to the extended-chain backbone crystals. Inelastic chain parts will crystallize as folded platelets of the shish kebab.

INTRODUCTION

The subject of producing polymers with ultrahigh modulus and strength has attracted considerable interest recently. Several new routes have been found that lead to a marked improvement in the molecular orientation and chain extension, and thereby, to better mechanical properties of polymers. Very high Young's moduli could be obtained by high-pressure extrusion of solid polymers,[1,2] hot drawing techniques,[1] simultaneous polymerization and crystallization,[3] solid-state polymerization of single crystals of monomers,[4] solidification of polymers exhibiting liquid crystalline behavior,[5] and crystallization of polymers in elongational flow fields.[6-8]

Our approach to the problem has been to reduce the number of structural and topological defects in crystalline polymers, such as folds, chain ends, and trapped entanglements, which lower the strength and the modulus. This is attempted by stretching very long-chain molecules in the course of crystallization under optimum conditions. Normally, polymer molecules crystallize at large degrees of supercooling in a lamellar habit containing an excessive number of defects, such as chain folds. Crystallization at low degrees of supercooling inevitably leads to more perfect solids. Our method, which has recently been developed,[8,9]

Journal of Applied Polymer Science, Vol. 26, 303–320 (1981)

0021-8995/81/0026-0303$01.80

allows crystallization to take place at temperatures close to and even above[8,10] the equilibrium dissolution temperature.[11,12] This technique is a variant of the well-known Czochralski technique and consists of submerging a fibrous seed crystal in a slightly supercooled dilute solution of high-molecular-weight polyethylene, which is stirred by the inner cylinder of a Couette apparatus. The seed crystal slides along the surface of the rotating cylinder, and the growing fiber is wound up on a drum at a speed that is equal to the crystal growth rate. The ensuing polyethylene fiber had an extremely high modulus (up to 105 GPa) and tensile strength (up to 4 GPa[8]).

This article is the result of a further investigation into the crystallization of long-chain molecules in a stretched state along the rotor surface, a process which is referred to as "surface growth." It turned out to be a rather complex process involving the adsorption of the macromolecules on the rotor surface and the formation of an entanglement network by reptation of the chains through the loops of the absorbed molecules. This network, connected through cilia to the growing fibrous crystals, is stretched by the opposing motion of fiber and rotor.

Obviously, a further study of the mechanism underlying the formation of these interconnected fibrous crystals is a subject on its own. Moreover, such a study may also add to the understanding of other routes leading to the production of ultra-high modulus polymers and to the understanding of comparable processes, such as spinning and subsequent drawing of gels.[13,14]

In the following pages, we describe first the most conspicuous experimental observations; secondly, the mechanism of the "surface growth" is presented; and finally, some remarks are made regarding the relation between this mechanism and the resulting fiber structure.

EXPERIMENTAL

Materials

The surface growth technique is described in more detail in previous work.[9] The linear polyethylene used had, according to the supplier (Hercules), a weight-averaged molecular weight of 4.10^6 g/mol. This polymer was dissolved at a concentration of 4.29 g/liter of solvent. High-purity solvents *p*-xylene, *n*-dodecane, decahydronaphthalene (decalin), and paraffin oil (viscosity at 20°C: 70 cP) were used. All polyethylene solutions were stabilized by 0.5% by weight of the antioxidant ditertiary-butylparacresol and were kept under purified nitrogen, in order to prevent oxidative degradation. The solvent *p*-xylene was used, except where otherwise indicated.

Couette Instruments

The Couette instruments used throughout this investigation comprised an inner cylindrical stirrer (rotor) with a diameter of 115 mm and an outer cylinder of 130 mm. The dimensions of a second instrument were 179 mm for the diameter of the inner cylinder and 191 mm for the outer cylinder. We have also used an instrument with a rotor with horizontal axis having a diameter of 117 mm as is described earlier[15] in more detail.

Rotors of PTFE (Teflon), glass, and covered with a tungsten foil were used. The surfaces were polished with polishing paper, which was covered with 15-μm particles, or were sandblasted with particles of corundum with a distribution in diameter ranging from 30 to 110 μm. In some cases, the Teflon rotors were modified with a wedge-shaped groove, which was 0.5–1.0 mm deep and had an angle of 60° or 90°. The instrument was submerged in a temperature-regulated oil bath, which was controlled within ±0.05°C.

Fiber Cross Section

The cross section of the fibers was usually determined, under exclusion of pores, by dividing the mass per unit length by the density of 1000 kg/m^3. The dimensions of the fiber, including the pores, were determined by means of light microscopy and scanning electron microscopy.

Take-Up Force

The take-up force was measured by means of a Statham strain gauge (model UC-3). Details of the operating procedure[16] and accessories for this transducing cell have been described elsewhere.

Hot Drawing

One surface growth fiber was subjected to a hot drawing process, which has been described earlier.[17] The fiber was drawn with a draw ratio of 5 in a nitrogen atmosphere at 150°C under conditions of constant force.

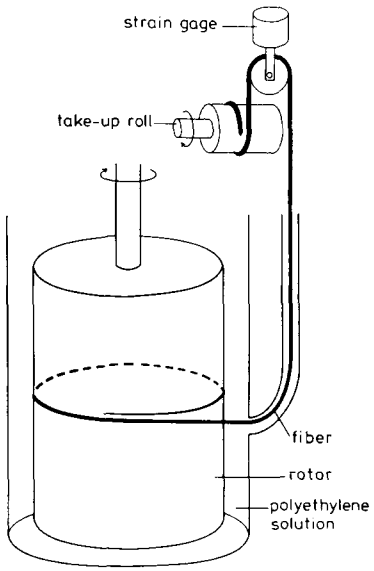

Fig. 1. Schematic representation of fiber growing on cylindrical rotor submerged in polyethylene solution.

RESULTS AND DISCUSSION

General Description of Surface Growth Process

Figure 1 is a schematic representation of a surface growth apparatus consisting of an inner and outer cylinder. The inner cylinder (rotor) rotates in a dilute solution of high-molecular-weight polyethylene in the direction indicated by the arrow. Fiber growth is initiated by letting a seed fiber make contact with the rotor. A fiber then grows from the seed fiber in the direction in which the rotor moves.

Seed and growing fiber are wound up continuously, on a take-up roll, and pass over a strain gauge, which measures the take-up force. If the take-up speed matches the longitudinal growth rate of the fiber, a continuous filament can be produced for weeks resulting in, for example, a length of up to 10 km.

The course of the process is watched by means of the assessment of the cross section and the stress of the fiber. The cross section is related to the growth rate of the fiber in lateral direction, and the stress is related to the coil deformation.

Knowledge of the morphology and the structure of the fiber is obtained by wide and small angle x-ray diffraction and by electron microscopy, and yields information about the crystallization process. Some of the most important process variables are the temperature of crystallization, the rotor speed, and the take-up speed.

The most conspicuous observations on the crystallization process from which the picture of the mechanism is deduced are given in the next sections.

Fiber in Gel Layer

It has been reported that a gel layer adhering to the rotor surface can be observed.[15] This observation was made using a rotor with an horizontal axis. The rotor was only partly submerged in the polymer solution. The part of the rotor surface above the solution level was in all cases covered with a viscous and transparent layer with a thickness of about 0.5 mm. It was possible to keep a fiber growing continuously even with only 10% of the rotor's diameter submerged. The fiber was also growing at the rotor part above the solution level.

These observations indicate that the conditions for the formation of a gel layer are also required for surface growth. This conclusion is confirmed by measurements of Barham et al.,[18] who studied gelation of the solution upon cooling and the possibility of surface growth.

In some cases, a fiber was covered with a gel-like layer as it was pulled out of the Couette apparatus. It is very likely that this gel originates from the gel on the rotor surface. After extraction of the solvent, scanning electron microscopy revealed that the gel adhering to the fiber consisted of oriented fibrils covered with large lamellae, as shown in Figure 2. This oriented gel has the typical shish kebab stucture of the surface growth fibers. However, the lamellae have, in the case of the gel, a diameter of about 1 μm, whereas they are considerably smaller in diameter in the case of a fiber. Figure 3 shows a fiber having lamellae of about 0.1 μm. The smaller lamellae of the fiber point to a larger degree of extension

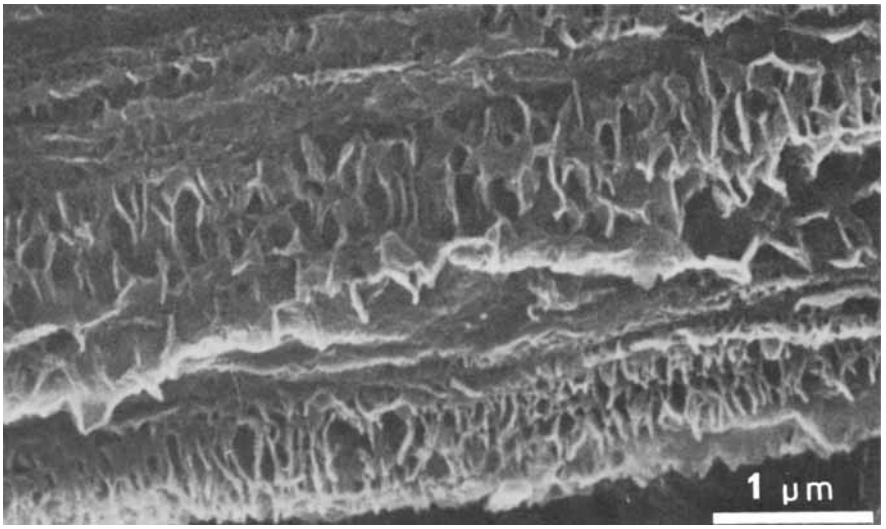

Fig. 2. Scanning electron micrograph of dried gel of polyethylene showing fibrils with skish kebab morphology. Kebab diam: 1 μm (polished Teflon rotor, 115-mm diam; temperature of crystallization, 125°C; rotor speed, 66.7 mm/sec; take-up speed 2.33 mm/sec; solvent, paraffin oil).

of the constituting polymer molecules. The gel adhering to the fiber may have achieved fibrillar morphology by extension of its precursor, which is the layer on the rotor. But the fibers must have grown under extreme conditions; these conditions may be met close to the surface of the rotor, as will be shown in the next section.

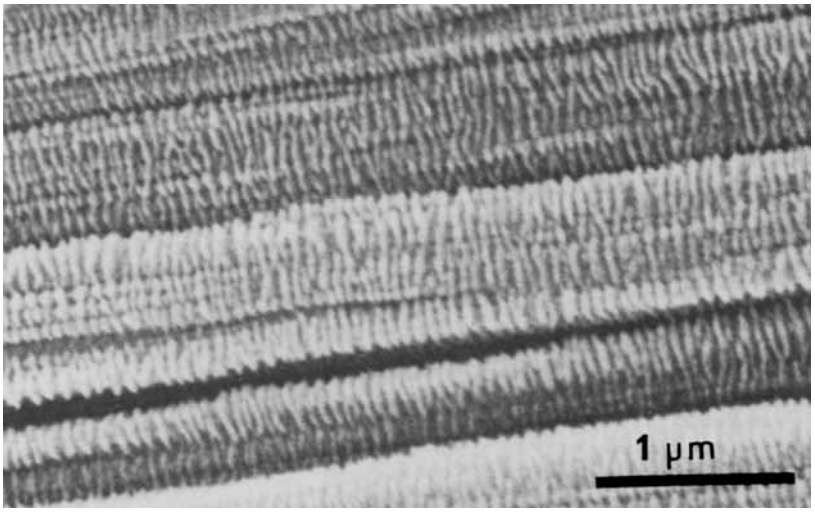

Fig. 3. Scanning electron micrograph of surface growth fiber showing fibrils with shish kebab morphology. Kebab diam: ~0.1 μm. (Teflon rotor, 115-mm diam; temp. of crystallization, 114°C; rotor speed, 71 mm/sec; take-up speed, 0.53 mm/sec).

Adsorption and Gel Layer

The roughness and the chemical nature of the rotor surface, as well as the solvent quality, influence the cross section of the fibers which are crystallized under set process conditions, (e.g., rotor speed and supercooling). The cross section is, however, also influenced by another parameter, the take-up speed.

Characteristic of the process and regardless of the take-up speed is "the mass of fiber produced per unit time" (shortly, the crystallized mass W) and it will be used for comparison of different process conditions.

In Table I, it is shown that the crystallized mass W increased as the roughness of a Teflon surface increased. After a further increase in roughness, the crystallized mass decreased again. Furthermore, when a tungsten surface was used, the crystallized mass was five times smaller than with a Teflon surface, even though the surface finishes were similar. The influence of the solvent quality is reflected in the results from experiments with p-xylene, resulting in a crystallized mass of 2.30 μg/sec, and with decahydronaphthalene, resulting in a crystallized mass of only 0.25 μg/sec at similar supercooling and other process conditions.

Earlier results,[9] in which an apolar coating had been deposited on a glass surface, resulted in an increased crystallized mass. At that time, adsorption of the apolar polyethylene molecules was already suggested as a possible explanation. The present results also suggest strongly that adsorption plays an important role in surface growth, as will indeed be shown later.

Adsorption must be discussed in terms of competition between the solvent and the polymer segments for an adsorption site.[19] Thus, the difference in interaction energy between solvent molecules and segments with the adsorbens, is essential,[20] but also the interaction between solvent and polymer must be taken into account.

In the case of tungsten, the adsorption energy of the solvent p-xylene will be larger because of its polarizable π-bond system, which interacts with the electric double layer[21] of the metal. p-Xylene is thus a good competitor and, therefore, polyethylene will adsorb only weakly on tungsten. For PTFE rotor surfaces, the reverse holds true. Sorption measurements indicated that molecules with π-bonds (as in the case of the solvent used), interact less strongly with PTFE than do saturated molecules, such as polyethylene. Thus, absorption of polyethylene will be great on PTFE, but small on tungsten. Table I shows that the crystallized mass W is great with PTFE, but small with tungsten. Coombes and Keller[22] have found a similar behavior pattern in the surface growth of films, a process comparable to that of fiber formation. The crystallized mass was greater

TABLE I
Influence of Rotor Surface on W, the Mass of Fiber Produced per Unit Time[a]

Rotor surface	W, (μg/sec)
Teflon	
polished	0.71
lightly sandblasted	1.68
intensively sandblasted	0.36
Tungsten	
polished	0.13

[a] Cylindrical rotor, 115-mm diam; temp. of crystallization, 113°C; rotor speed, 68 mm/sec.

with PTFE than with metals such as brass and steel, as can be calculated from their data.

The solvent quality influences adsorption as well. Strong interaction of the solvent with the polymer segments reduces the interaction of the polymer with the adsorbens. It is known that decahydronaphthalene interacts more strongly with polyethylene than *p*-xylene[23] does.

Adsorption of the polymer will, therefore, be stronger in the case of *p*-xylene. As mentioned earlier, the crystallized mass is about ten times bigger with *p*-xylene used as a solvent than with decahydronaphthalene.

Thus, it was found several times that a stronger adsorption of polyethylene results in a larger amount of fiber produced per unit of time (W). This conclusion will have a profound bearing on our view of the mechanism of fiber formation.

The increase of crystallized mass, matching an increase in roughness (Table I), is in accordance with this conclusion. This is true because, with an increase in surface roughness, there is a simultaneous increase in effective surface area and a consequent increase in the amount of adsorbed polymer. A further increase of crystallized mass, when the surface is made rougher still, is indicative of another phenomenon. It may very well be that in the case of a very rough surface, a fiber sliding across that surface can only use the tops of the asperities, so that the effective surface area becomes much smaller. This indicates that the growth process takes place very close to the surface.

At this moment, it is necessary to elucidate the relation between the formation of the gel layer and the adsorption of the polymer.

The gel layer with a thickness of 0.5 mm, which adheres to the rotor surface, may consist of several layers. At the surface, polymer molecules are adsorbed in a loop-train-tail manner by multiple points of physical adsorption.[24–26] The solution concentration is higher than the critical entanglement concentration. Therefore, other molecules are entangled through the loops of the adsorbed molecules, so that a multilayered network of entangled molecules is firmly bound to the rotor. The thickness of this network cannot, by far, amount to the observed value of 0.5 mm. Measurements of the Weissenberg effect[27] indicate that in the solutions used for surface growth, flow-induced crystallization occurs. The crystalline structures so-formed, which are covered with a fuzz of dissolved chains, will form a network on the rotor surface.[28] This is confirmed by measurements of the deposition of polyethylene on teflon foils[18] which are submerged in the solution in a Couette apparatus.

In this way, a second layer of the gel is formed. A third layer of the gel may result from the general phenomenon of liquids adhering to surfaces that are dipped in these liquids.[29,30]

Lateral Growth

Figure 4 shows a scanning electron micrograph of a twisted fiber. Owing to the twisting, it can be easily observed that the fiber has the shape of a ribbon. This ribbon shape is observed in almost all cases. The thickness of the ribbon ranges usually between 15–25 μm; whereas the width depends on the conditions of crystallization and ranges from 20 to 600 μm. The shape of the fiber clearly indicates that it does not grow equally fast in all directions.

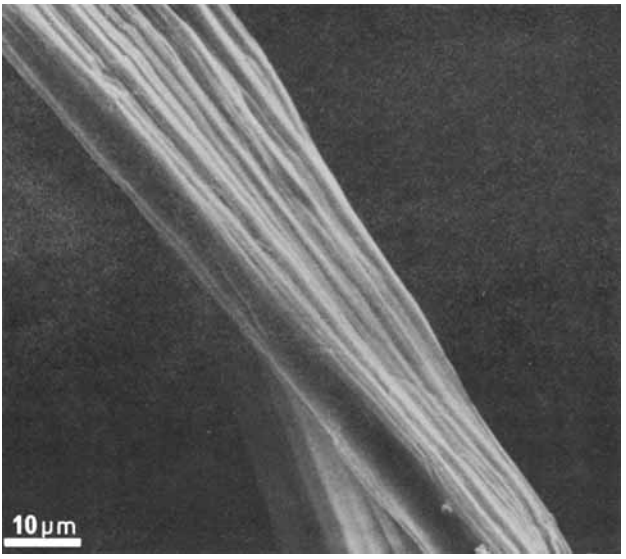

Fig. 4. Scanning electron micrograph of twisted polyethylene fiber. Ribbon shape is evident (polished Teflon rotor, 115-mm diam; temperature of crystallization, 110°C).

It is observed that the ribbon grows with its broad side parallel to the rotor surface. In Figure 5, the width and thickness of the ribbon are plotted versus reciprocal take-up speed. The reciprocal take-up speed is a measure of the period of time during which the fiber remains in contact with the rotor; when the fiber is wound up twice as fast, it takes only half as long for the fiber to slide over one rotor circumference. Figure 5 shows that the width increases with the reciprocal take-up speed, and thus with the period of residence, while the thickness remains constant. This feature indicates that the fiber grows in width primarily. This phenomenon will be referred to as lateral growth.

One would expect the take-up force during fiber growth to be large, under those experimental conditions which result in a large fiber cross section. However, Figure 6 shows that the take-up force is almost independent of cross section (at

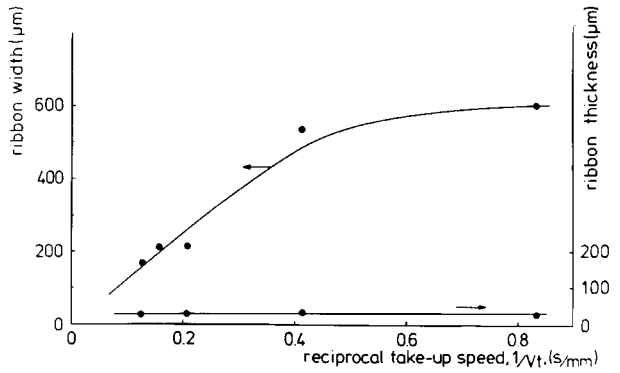

Fig. 5. Width and thickness of ribbon-shaped polyethylene fiber plotted against reciprocal take-up speed (Teflon rotor with horizontal axis, diam 117 mm, with groove; temp. of crystallization: 123°C; rotor speed, 208.7 mm/sec; solvent, *n*-dodecane).

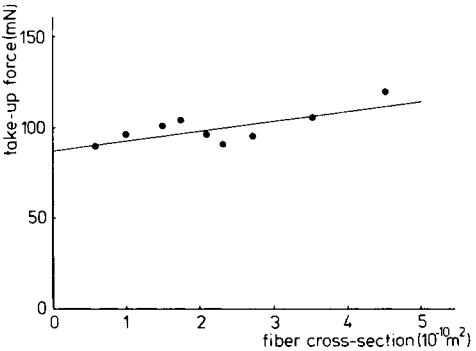

Fig. 6. Take-up force vs. fiber cross section (Teflon rotor, diam 115 mm, with groove; temp. of crystallization, 113°C; rotor speed, 50.5 mm/sec; take-up speed, 1.63–8.33 mm/sec).

least in the case of a grooved rotor surface). The force arises primarily from the friction between the fluid and the fiber and not from the friction between the rotor surface and the fiber, as is indicated by measurements of frictional force in pure solvent and in a 0.5% EPDM/rubber solution.[8] It is well known that in the entangled solutions used for surface growth, the chain entanglements constitute the largest part of the viscous friction.[31] Hence, the take-up force must be directly proportional to the number of entanglements holding on to the fiber. This number must, therefore, be almost independent of the cross section of the fiber. This indicates that these entanglements must be formed with the constant lateral surface of the fiber. One may therefore expect that only at the lateral surface can molecules be deformed to such a degree that they are able to crystallize in extended-chain crystals. This suggests growth at the lateral surfaces of the fiber.

Wide-angle x-ray diffraction experiments have revealed that the crystals in the fiber are oriented with their c axis along the fiber direction as has been published before.[32] Furthermore, we have recently observed, by means of WAXS experiments, that the a and b axes also are not randomly distributed, but are preferentially oriented in the plane pependicular to the fiber axis. The crystals are presumably similarly oriented as stirring-induced polyethylene crystals.[33] In these crystals, the normal to the ribbon plane is parallel to the crystallographic a axis. These observations are in accordance with growth in one direction, such as lateral growth.

Shape of Growing Fiber

It has been observed in many cases that the fiber growing in the Couette apparatus lies approximately one circumference around the rotor. This situation is represented in Figure 1. This peculiar constancy of the length is explained by an intrinsically high-longitudinal growth rate of the fiber, combined with a self-regulating mechanism becoming active at a fiber length of one circumference. These phenomena will be dealt with in a future article. Using a rotor of glass, allowing for easy visual observation, it was realized that the fiber had a tapered shape. Measuring further away from the take-up apparatus, the ribbon becomes gradually less wide; it reaches a minimum value at its tip. A similar tapered shape was also found for fibers grown in a Poiseuille flow[34] in our laboratory and

by McHugh, Ejike, and Silebi,[35] who explained the shape, in their case, as an entrance region effect.

Further investigation into the tapered shape was carried out by stopping the rotation, which caused the crystallization to stop as well. Then the fiber was carefully withdrawn from the solution and dried. In this manner, it was possible to determine the shape of the incompletely grown fiber. (Although the cross section during growth is different from that of the dry fiber, its shape should be essentially retained.) Figure 7 displays the width of the ribbon plotted against the distance to the take-up apparatus, (an arbitrarily chosen reference point).

The thickness of the ribbon was more or less constant at 15 μm. The value of 40 μm in the left half of Figure 7 is the steady value of the fiber that has grown normally. The peak in the curve is due to contraction of the fiber, at the moment when the stress drops to zero, because the rotation has been stopped. The descending straight line in the right-hand part of the figure corresponds to the part of the fiber in contact with the rotor at the moment when growth was interrupted. This line shows that growth does not take place at the fiber tip only, but that the width of the ribbon increases over the whole length with which it makes contact with the rotor, at a more or less constant rate.

Extra Evidence for Lateral Growth

From the results as described in the previous section and in particular from the approximately straight line in Figure 7, it can be concluded that the lateral growth rate is constant over the entire rotor circumference. Using this feature, it is possible to deduce an equation for W, the mass of fiber produced per unit of time:

$$W = 2\rho \cdot l \cdot h \cdot G_{LAT} \qquad \text{(kg/sec)} \tag{1}$$

where ρ is the density of the dry polyethylene fiber (kg/m^3), l is the length of the wet fiber in contact with the rotor over which lateral growth takes place (m), h is the thickness of the dry ribbon-shaped fiber (m), and G_{LAT} is the rate at which the width of the ribbon increases (m/sec).

As noted before, l is in most cases approximately equal to one rotor circumference: $\pi \cdot D$, where D is the diameter of the rotor. The thickness of the ribbon, h, is in most cases approximately equal to 15 μm.

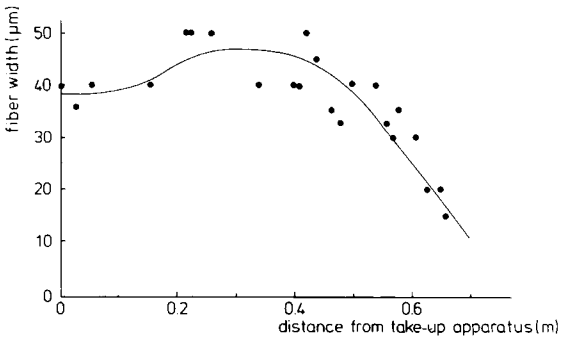

Fig. 7. Width of fiber vs. distance from take-up apparatus (polished Teflon rotor, diam 115 mm; temp. of crystallization, 113.5°C; rotor speed 52.8 mm/sec; take-up speed, 2.17 mm/sec).

It can be seen from eq. (1) that W, the crystallized mass, is independent of the take-up speed. With this equation, it is possible to calculate crystal growth rates from measurements of the crystallized mass, W, which is easily accessible in experiments. It is readily apparent that the amount of crystallizing fiber, W, is equal to the amount wound on the take-up roll. The latter amount is directly proportional to the density and cross section of the fiber, as well as to the take-up speed. This results in the following equation:

$$W = \rho \cdot V_t \cdot \phi_c \qquad \text{(g/sec)} \tag{2}$$

where V_t is the take-up speed and ϕ_c is the fiber cross section. By equating formulas (1) and (2), we get the following equation for the fiber cross section:

$$\phi_c = \frac{2\pi D \cdot h \cdot G_{LAT}}{V_t} \qquad (\text{m}^2) \tag{3}$$

Generally, the thickness of the ribbon, h, varies only slightly. Under constant crystallization conditions, such as temperature and rotor speed (among others), the lateral growth rate, G_{LAT}, is constant; and, therefore, the fiber cross section should be directly proportional to the reciprocal take-up speed:

$$\phi_c \sim \frac{1}{V_t} \tag{4}$$

Such experiments have been carried out by changing only the take-up speed. The expected direct proportionality is indeed found as is displayed in Figure 8. This result is in accordance with the lateral growth. It would not be in accordance with growth of the fiber at its tip only, immediately with the final cross section. Fibrous growth at different take-up speeds would instead lead to a constant cross section, and therefore, to the horizontal line in Figure 8.

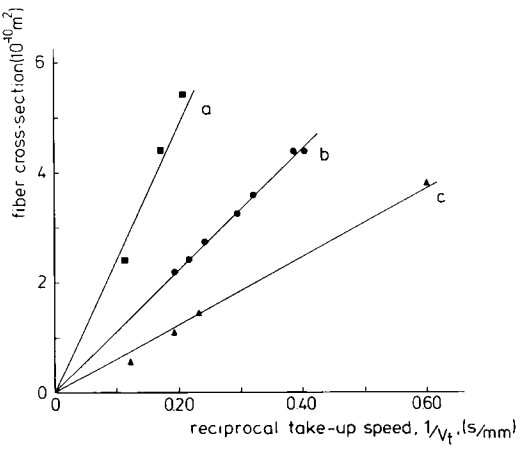

Fig. 8. Cross section of fiber vs. reciprocal take-up speed at several conditions of crystallization (polished Teflon rotor, diam 115 mm; temperatures of crystallization and rotor speeds: 110°C, 120 mm/sec; 110°C, 89 mm/sec; 113°C, 50.5 mm/sec, respectively).

Mechanism

The most conspicuous results leading to our picture of the mechanism of fiber formation have now been presented. Using these results, we will now proceed to discuss the mechanism itself.

Adsorbed Molecules in Contact with Fiber

Figure 9(a) shows a "development." The development is achieved in an imaginary experiment in which the surface of the rotor is peeled off and forced in the shape of a plane. The fiber and the gel layer, which move in opposite directions, are indicated. For the sake of clarity, the fiber has been drawn several times wider and also more strongly tapered than in actual fact. Figures 9(b) and 9(c) are cross sections of the fiber and gel layer. Below the fiber, no polymer is available and the fiber makes contact with the rotor, as is clear from the ribbon shape of the fiber and by the formation of uniform films on the slightly tapered rotor.[22] At the entire lateral surface of the fiber, polymer molecules are available, viz., those in the gel layer. From the results concerning adsorption of polyethylene on the rotor surface (section adsorption) and from the relative height of the fiber (less than 25 μm) as opposed to the height of the gel (500 μm), it is assumed that only the lower layers of the gel are requisite for crystallization. These layers are presented in Figure 10, a more detailed drawing of Figure 9(b). The lower layers of the gel consist of polymer molecules adsorbed in loop-train-tail manner. With these loops the few next layers of molecules are entangled, and thus connected rather firmly to the rotor surface. The fiber is covered with partly dissolved emanating chains or cilia. By reptation, these cilia will form entanglements with surrounding molecules such as those in the adsorbed and entangled layers of the gel.

Extension of Entangled Network

Entangled molecules are suitable for extension.[36] This becomes evident when observing clusters of entangled molecules of polystyrene in Couette flow.[37–39] In the case of molecules which are connected to a surface, a shearing action is sufficient to induce extension and eventually crystallization.[40]

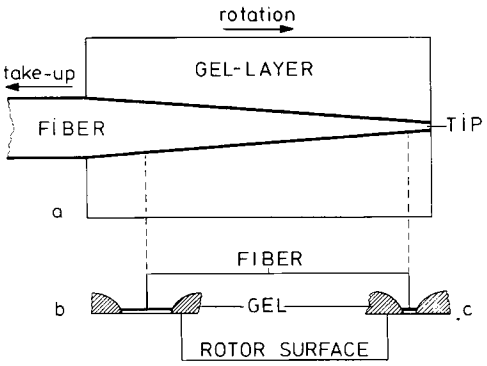

Fig. 9. Schematic representation of growing fiber in contact with gel layer and rotor surface: (a) development, (b) and (c) schematic drawings of view tangent to rotor; (b) close to where the fiber is pulled off rotor; (c) close to tip of fiber.

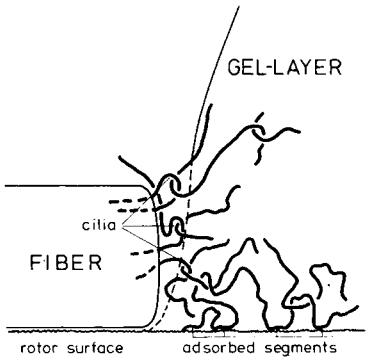

Fig. 10. Schematic cross section of growing fiber in contact with molecules near rotor surface. Molecules adhere to rotor surface because of trains of adsorbed segments. Subsequent layers of molecules form entanglements with loops of adsorbed molecules and cilia dangling out of crystalline fiber. Rotor and adsorbed molecules move into plane of paper; fiber moves in opposite direction.

Because of the shear flow between rotor and fiber in the surface growth method, the network of adsorbed molecules becomes extended. Great Weissenberg effects[27] suggest that in such a network small, temporary crystallites exist when the network is deformed. This hetero phase-fluctuation phenomenon[41] is illustrated in Figure 11. This figure shows a network of entangled molecules in which, after the application of stress, small embryonic crystallites[42–44] are formed. The formation of these crystallites is, at least partly, explained by the increase in the free energy of coiled molecules, when they are deformed.[45,46] This higher free energy induces crystallization.

A consequence of the formation of these embryonic crystallites is a considerable increase in the relaxation times of the entanglements so that their release is prevented. On account of this phenomenon, further extension of the network to a very high degree is possible, with crystallization proceeding in chain-extended conformation. In this rapid process, many "defects" existing in the solution will be trapped as crystal defects, e.g., trapped entanglements, folds, kinks, twists, and chain ends.

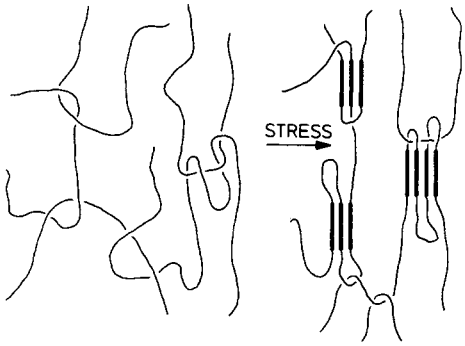

Fig. 11. A network of entangled molecules in supercooled state results in embryonic crystallites (thick lines) when stress is applied.

Moreover, molecules still being part of the entangled network will be built into the crystallites which constitute the fiber. From this it follows that the network is continuously drawn towards the fiber. The network is thus creeping over the rotor surface towards the fiber. This requires that some entanglements be released, while new ones are formed with the loops of adsorbed molecules by processes like reptation.[47] In this way, the molecules near the rotor surface always have a relaxation time that is long enough to allow for substantial extension.

Experiments have indicated that the rate of fiber formation (equal to W, the crystallized mass) increases if the temperature is lowered[8] and if the rotor speed is increased. This suggests that fiber formation is determined by the free energy of crystallization, which energy itself determines the rate of crystallization. The dependence of the process on the rate of crystallization can be explained through the trapping of the polymer molecules in crystallites: if crystallization takes place at too slowly a rate, the molecules can slip out of entanglements and are lost for incorporation into the fiber.

However, the slipping of molecules along each other and similar phenomena of creep can be beneficial, because creep will allow for stress relaxation. This is reflected in the higher tensile strength of fibers grown at higher temperatures,[48] or more generally at higher stresses. In the first place, creep occurs more easily at a higher temperature, and in the second place, stress will be higher because further extension of molecules is required before their elastic free energy is high enough for crystallization to take place.

The supply of molecules over macroscopic distances throughout the Couette apparatus towards the place of crystallization, may occur by higher-order flow phenomena.[49] Vortices similar to the Taylor vortices that have been observed earlier,[42] were indeed observed in p-xylene solutions under all experimental conditions used for surface growth in this work.

Additional Remarks on the Mechanism

The increase in fiber formation rate (W) with a corresponding increase in the amount of polymer adsorbed on the rotor surface (section on adsorption) suggests the following: A larger quantity of adsorbing polymer segments causes the polymer chains to adhere more strongly to the surface; this effect of stronger adherence will extend into a few entangled layers. Hence, more molecules will be able to sustain the great tensile forces required for their extension and the crystal growth rate will increase. The decrease in fiber formation rate on a very rough surface may be due to a surface morphology of "mountains and valleys." The molecules above the "valleys," are far away from the adsorbed molecules; therefore, they are only indirectly and less strongly connected to the rotor. Hence, these molecules will have shorter relaxation times in their entanglements towards the rotor and will not be sufficiently deformed. This may explain why surface growth must take place close to the rotor surface.

The observed continuous structure of the fiber is explained in this mechanism by molecules extending through several crystallites. This happens because the molecules are about a factor of 1000 longer tnan the crystallites.

It would be worthwhile to estimate the effect of stress-induced diffusion[50,51] on the surface growth process; however, these estimates have not been made by us.

Crystallized Entanglement Network

Several features of the structure and morphology of the fiber have been reported previously,[32] and new results will be presented in this section. The question arises whether this structure is in accordance with what would be deduced from the underlying mechanism.

From earlier work,[32] it is known that the fiber consists of elementary fibrils in which crystalline regions are interspaced with regions containing crystal defects. Now it is observed that a fiber crystallized at a high temperature contracts very rapidly, and even seems to form a droplet, when it breaks during growth (at 127 and 129°C in *n*-dodecane, which has a equilibrium dissolution temperature of 128.5°C). This is indicative of the superheated state of the crystals, which dissolve as soon as the stress is released, which is caused by fracture. The peak in Figure 7 also indicates such a contraction when the stress is released. The degree of contraction seems to depend on the temperature.

At the crystallization temperature, the defect regions can be considered being amorphous and molecules in these regions must be highly mobile. However, the fibers can sustain take-up stresses up to 40% of their strength at room temperature. This high strength can only be due to tie molecules and entanglements bridging the otherwise weak, disordered regions. The existence of these tie molecules and entanglements has also been deduced from the increase in the apparent dissolution temperature by 13°C of a fiber subjected to stress.[52] Also, blended fibers of polyethylene and polypropylene produced by the surface growth technique[53] contain intimately mixed crystalline regions of each pure component. This is indicative of crystallization of the network, retaining all topological "defects," as they occur in the solution.

While being cooled off to room temperature, the width of the fiber decreases by a factor of at least 2 or 3. This lateral contraction points to the existence of lateral tie molecules between different fibrils. Normally, these lateral connections cannot be discerned on scanning electron microscopy photographs. When the fibers are being subjected to the process of hotdrawing,[17] however, the connections between fibrils become visible, as is shown in Figure 12.

Figure 13 is a schematic drawing of the fiber structure at crystallization temperature containing all features that were discussed previously. This structure is in accordance with the mechanism in which an entanglement network crystallizes. The elastically effective chains of the network will form extended-chain molecules which will constitute the crystallites in the backbones. Elastically ineffective chain parts will form cilia at a high temperature, which will, at a lower temperature, crystallize as lamellae on the backbones.[54] Crystal growth at high temperature, which is accompanied by high stress and rapid creep in the network, will result in a greater fraction of elastically active chains. The smaller fraction of elastically inactive chain parts will result in less cilia, and hence, in fibers with smaller lamellae, as has indeed been observed.[48]

The result, the shish kebab structures being formed by extension of a physical network (as has been suggested earlier[28]), does not come as a surprise. It has been shown that chemically crosslinked networks can lead to the formation of shish kebabs, when the networks are subjected to strain-induced crystallization.[55]

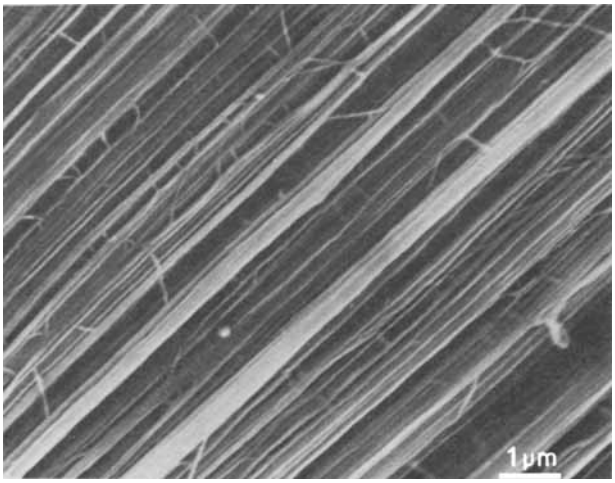

Fig. 12. Scanning electron micrograph of hot-drawn surface growth fiber of polyethylene, depicting long fibrils oriented in fiber direction and their connections (fiber grown on Teflon rotor with groove, with horizontal axis, diam 117 mm; temp. of crystallization, 123°C; rotor speed, 120 mm/sec; take-up speed 0.48 mm/sec; solvent, *n*-dodecane. Hot drawing carried out at 150°C).

CONCLUSIONS

The mechanism underlying the formation of the ultrahigh strength and modulus fibers of polyethylene, by means of the surface growth technique, can be summarized as follows:

Polymer molecules are adsorbed onto the rotor surface with loops extending into the solution. By reptation, other molecules become entangled with those loops and with each other. Thus, a network with physical crosslinks adheres to the surface of the rotor. The lateral surface of the ribbon-shaped fiber, is covered with cilia (partly dissolved chains). By reptation, these become entangled with the physical network. Owing to the shear between rotor and fiber, the network is extended and embryonic crystals are formed. These greatly increase the relaxation times of the entanglements so that creep is limited, and hence, allow for extreme extension of the macromolecules.

However, the limited degree of creep which still takes place tends to result in an equal distribution of stress over all chains which traverse a fiber cross section.

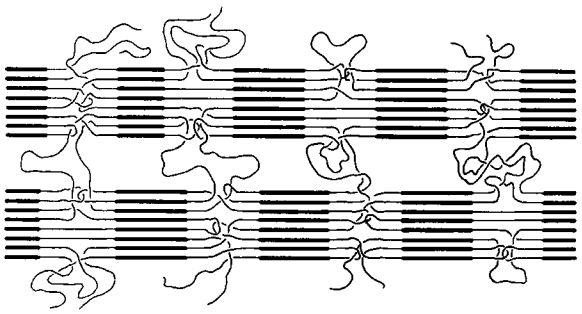

Fig. 13. Polyethylene fiber at crystallization temperature (110°C) in solvent. Crystalline regions (thick lines) are interspaced by large amorphous parts, which are bridged by tie molecules and trapped entanglements. Interfibrillar tie molecules and cilia emerge from amorphous zones.

Therefore, the fiber attains a more perfect structure with better mechanical properties. This results in further extended-chain crystallization of the network.

In this process of extension and crystallization, the elastically active chains will form the extended-chain backbones, while the elastically inactive chains will constitute the lamellar crystals.

At higher crystallization temperatures, the chains have to be extended further before crystallization can take place, and thus, the amount of stress is higher and smaller lamellae are formed, resulting in stronger fibers.

The authors gratefully acknowledge the suggestions made by Prof. Dr. Ir. A.A.H. Drinkenburg and are indebted to B. A. Klazema for the electron microscopy work.

References

1. G. Capaccio, A. G. Gibson, and I. M. Ward, in *Ultra-High Modulus Polymers*, I. Ward and A. Ciferri, Eds., Applied Science, Barking, Essex, England, 1979.
2. A. E. Zachariades, W. T. Mead, and R. S. Porter, in *Ultra-High Modulus Polymers*, I. Ward and A. Ciferri, Eds., Applied Science, Barking, Essex, England, 1979.
3. M. Iguchi, *Br. Polym. J.*, **5**, 195 (1973).
4. G. Wegner, *Faraday Discuss. Chem. Soc.*, **68**, (1979).
5. J. Preston, in *Ultra-High Modulus Polymers*, I. Ward and A. Ciferri, Eds., Applied Science, Barking, Essex, England, 1979.
6. A. Keller, in *Ultra-High Modulus Polymers*, I. Ward and A. Ciferri, Eds., Applied Science, Barking, Essex, England, 1979.
7. A. J. Pennings, *J. Polym. Sci. Polym. Symp.*, **59**, 55 (1977).
8. A. J. Pennings and K. E. Meihuizen, in *Ultra-High Modulus Polymers*, I. Ward, A. Ciferri, Eds., Applied Science, 1979.
9. A. Zwijnenburg and A. J. Pennings, *Colloid. Polym. Sci.*, **254**, 868 (1976).
10. P. J. Barham and A. Keller, *J. Polym. Sci., Polym. Lett. Ed.*, **17**, 591 (1979).
11. J. F. Jackson, L. Mandelkern, and O. C. Long, *Macromolecules*, **1**, 218 (1968).
12. A. J. Pennings, J. M. M. A. van der Mark, and A. M. Kiel, *Kolloid. Z. Z. Polym.*, **237**, 336 (1970).
13. B. Kalb and A. J. Pennings, *Polym. Bull.*, **1**, 871 (1979).
14. P. Smith, P. J. Lemstra, B. Kalb, and A. J. Pennings, *Polym. Bull.*, **1**, 733 (1979).
15. A. J. Pennings and J. C. Torfs, *Colloid. Polym. Sci.*, **257**, 547 (1979).
16. A. Posthuma de Boer and A. J. Pennings, *Macromolecules*, **10**, 981 (1977).
17. J. Smook, J. C. Torfs, P. F. van Hutten, and A. J. Pennings, *Polym. Bull.*, **2**, 293 (1980).
18. P. J. Barham, M. J. Hill, C. G. Cannon, and A. Keller, *Faraday Discuss. Chem. Soc.*, **68**, 120 (1979).
19. (a) G. Howard and P. McConnel, *J. Phys. Chem.*, **71**, 2974 (1967); (b) ibid., 2981; (c) ibid., 2991.
20. B. G. Belenkii, *Pure Appl. Chem.*, **51**, 1519 (1979).
21. J. C. P. Mignolet, *Faraday Discuss. Chem. Soc.*, **8**, 105 (1950).
22. A. Coombes and A. Keller, *J. Polym. Sci., Polym. Phys. Ed.*, **17**, 1637 (1979).
23. A. Y. Coran and C. E. Anagnostopoulos, *J. Polym. Sci.*, **57**, 13 (1962).
24. M. Rosoff, in *Physical Methods in Macromolecular Chemistry*, Vol. 1, B. Carroll, Ed., Marcel Dekker, New York, 1969, pp. 22–35.
25. F. W. Rowland, R. Bilas, E. Rothstein, and F. R. Eirich, *Ind. Eng. Chem. Fundam.*, **57**, 46 (1965).
26. R. R. Stromberg, D. J. Tutes, and E. Passaglia, *J. Chem. Phys.*, **69**, 3955 (1965).
27. A. J. Pennings, H. C. Booij, and J. H. Duysings, *IUPAC Leiden*, Leiden, vol. 1, 1970, p. 263.
28. A. J. Pennings, *J. Polym. Sci. Polym. Symp.*, **59**, 55 (1977).
29. J. A. Tallmadge and C. Gutfinger, *Ind. Eng. Chem. Fundam.*, **59**, 19 (1967).
30. P. Groenveld, *Chem. Eng. Sci.*, **25**, 1267 (1970).
31. D. Soong and M. Shen, *J. Polym. Sci. Polym. Lett. Ed.*, **17**, 595 (1979).

32. A. Zwijnenburg, P. F. van Hutten, A. J. Pennings, and H. D. Chanzy, *Colloid. Polym. Sci.*, **256,** 8 (1978).
33. A. Keller and F. M. Willmouth, *J. Macromol. Sci. Phys.*, **6,** 539 (1972).
34. A. Zwijnenburg and A. J. Pennings, *Colloid. Polym. Sci.*, **253,** 452 (1975).
35. A. J. McHugh, E. Ejike, and C. A. Silebi, *Polym. Eng. Sci.*, **19,** 414 (1979).
36. G. Marrucci, *Polym. Eng. Sci.*, **15,** 229 (1975).
37. P. Munk and N. Nikolaeva, *J. Polym. Sci.*, **62**(174), S92–S94 (1962).
38. P. Munk and A. Peterlin, *Trans. Soc. Rheol.*, **14,** 65 (1970).
39. (a) P. Munk and A. Peterlin, *Rheol. Acta,* **9,** 294 (1970); (b) 288.
40. A. J. McHugh and E. H. Forrest, *J. Macromol. Sci. Phys.* **11,** 219 (1975).
41. J. Frenkel, "Kinetic theory of liquids," in *International Series of Monographs on Physics,* Oxford UP., Oxford, 1946.
42. A. J. Pennings, J. M. M. A. van der Mark, and H. C. Booij, *Kolloid. Z. Z. Polym.*, **236,** 99 (1970).
43. E. W. Fisher, M. Dettenmaier, M. Stamm, and N. Steidle, *Faraday Discuss. Chem. Soc.*, **68** paper No. 1, (1979).
44. A. A. Trapeznikov, *Colloid. J. U.S.S.R.*, **28**(5), 541 (1966).
45. G. Marrucci, *Trans. Soc. Rheol.*, **16,** 321 (1972).
46. D. Acierno, F. P. la Mantia, and G. Marrucci, *Polym. Eng. Sci.*, **18,** 817 (1978).
47. P. G. de Gennes, *J. Chem. Phys.*, **55,** 572 (1971).
48. A. Zwijnenburg and A. J. Pennings, *J. Polym. Sci., Polym. Lett. Ed.*, **14,** 339 (1976).
49. H. Giesekus, *Proceedings of the 4th International Congress on Rheology, Part 1,* Interscience, New York, 1965, p. 249.
50. M. Tirrell and M. F. Malone, *J. Polym. Sci., Polym. Phys. Ed.*, **15,** 1569 (1977).
51. C. A. Silebi and A. J. McHugh, *J. Polym. Sci., Polym. Phys. Ed.*, **17,** 1469 (1979).
52. J. C. Torfs, G. O. R. Alberda van Ekenstein, and A. J. Pennings, *Eur. Polym. J.*, to appear.
53. A. Coombes, C. G. Cannon, and A. Keller, *J. Polym. Sci., Polym. Phys. Ed.*, **17,** 1957 (1979).
54. A. J. Pennings, *J. Crystal Growth,* **48,** 574 (1980).
55. A. Posthuma de Boer and A. J. Pennings, *Faraday Discuss. Chem. Soc.*, **68** (1979).

Received May 22, 1980
Accepted June 27, 1980